Department of Pharmacy[1], Ningbo First Hospital, Ningbo; Institute of Drug Metabolism and Pharmaceutical Analysis[2], College of Pharmaceutical Sciences, Zhejiang University, Hangzhou; Gynecology Outpatient Department[3], Kaihua Maternal and Child Health Hospital, Quzhou, China

Metabolic interactions between flumatinib and the CYP3A4 inhibitors erythromycin, cyclosporine, and voriconazole

Jiangfei Chen[1,#,*], Suhang Guo[2,#], Xianzhu Yu[3], Jinxiu Lei[2], Tao Xu[1], Suyan Zhu[1], Lu Chen[2], Ping Xu[1], Xuan Zhou[1], Lushan Yu[2,*]

Received May 25, 2020, accepted June 6, 2020

**Corresponding authors: Jiangfei Chen, Department of Pharmacy, Ningbo First Hospital, Ningbo 315010, China*
chenjiangfei@163.com
Lushan Yu, Institute of Drug Metabolism and Pharmaceutical Analysis, College of Pharmaceutical Sciences, Zhejiang University, Hangzhou 310058, China
yuls@zju.edu.cn
[#]These authors contributed equally to this work.

Pharmazie 75: 424-429 (2020) *doi: 19.1691/ph.2020.0068*

Flumatinib, indicated for the treatment of Philadelphia chromosome-positive chronic myeloid leukemia, is a structural analog of imatinib and has shown higher potency than imatinib as a BCR-ABL inhibitor. In this paper, the metabolic profile of flumatinib was studied. It was found that CYP3A4 and CYP2C8 were the main cytochrome P450 enzyme substyles catalyzing the metabolism of flumatinib, and CYP3A4 has a stronger metabolic ability for flumatinib than CYP2C8. Erythromycin, cyclosporine, and voriconazole can inhibit the metabolism of flumatinib *in vitro*. Accordingly, co-administration of erythromycin and cyclosporine with flumatinib increased the plasma concentration and the systemic exposure of flumatinib in rats, which indicated that lower doses should be considered in clinical practice.

1. Introduction

Flumatinib is a selective inhibitor of BCR-ABL1 designed for treatment of Philadelphia chromosome-positive chronic myeloid leukemia in the chronic phase (CML-CP) and shows stronger inhibitory effects on the proliferation of target leukemic cells than imatinib treatment (Luo et al. 2010; Li et al. 2019; Yao et al. 2019). Flumatinib was approved for the CML therapy by the National Medical Products Administration of China in 2019. Flumatinib could also be a promising therapeutic agent against GISTs resistant to both imatinib and sunitinib because of secondary mutations in the activation loop (Zhao et al. 2014).

The main metabolites of flumatinib in humans were the products of N-demethylation, N-oxidation, hydroxylation, and amide hydrolysis (Gong et al. 2010). N-Desmethyl flumatinib (M1) and amide hydrolysis product (M3) are the two major metabolites in human plasma (Yang et al. 2012, Fig. 1). M1 has been demonstrated to exhibit pharmacodynamic activities similar to the parent drug. Other metabolites in the plasma comprised oxidation metabolites (M2-1, M2-4, M2-7, M2-9, and M14) and a hydrolysis metabolite (M4), which is further metabolized to form multiple metabolic products (M5, M6, M8-3, and M10) (Gong et al. 2010). However, metabolic enzymes involved in the metabolism of flumatinib and their metabolic profiles were both not reported.

Infections caused by various microorganisms are the most common complications in patients during all stages of leukemia and can seriously affect the remission and survival rate of leukemia patients (Yano et al. 1996). Therefore, the combined administration of antibiotics and flumatinib in clinic may result in interactions affecting the dosage, safety, and efficiency of flumatinib. Voriconazole (Asada et al. 2006; Bandettini et al. 2009) and erythromycin (Reich 1954) are commonly used during CML treatment in clinical settings. Furthermore, cyclosporine is used after HSCT in CML (Bandettini et al. 2009; Reich 1954). Therefore, the metabolic profiles of flumatinib mediated by cytochrome P450 enzymes and the drug-drug interactions between flumatinib and the above three drugs were studied in this study.

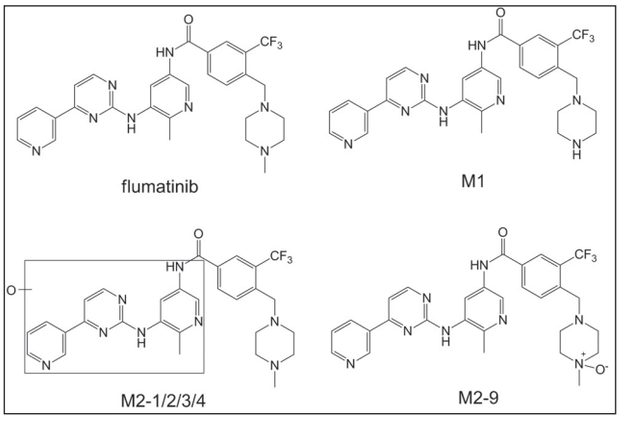

Fig. 1: Structures of flumatinib and its metabolites.

2. Investigations, results and discussion

2.1. Analytical evaluation

2.1.1. LC-MS/MS analysis

The representative chromatograms of flumatinib, M1, and the internal standard (IS) loratadine are shown in Fig. 2. Under the analysis conditions, the retention times of flumatinib, M1 and IS were 1.91, 1.93, and 2.14 min, respectively. The response of the interfering components was less than 20% of the lower limit of quantitation and less than 5% of the internal standard (n=6), which indicated that endogenous substances did not interfere with the determination of flumatinib, M1, and IS.

2.1.2. Calibration and linearity

The calibration curve was linear over the concentration range of 1.0-250 ng/mL of flumatinib and M1 in the rat plasma with correla-

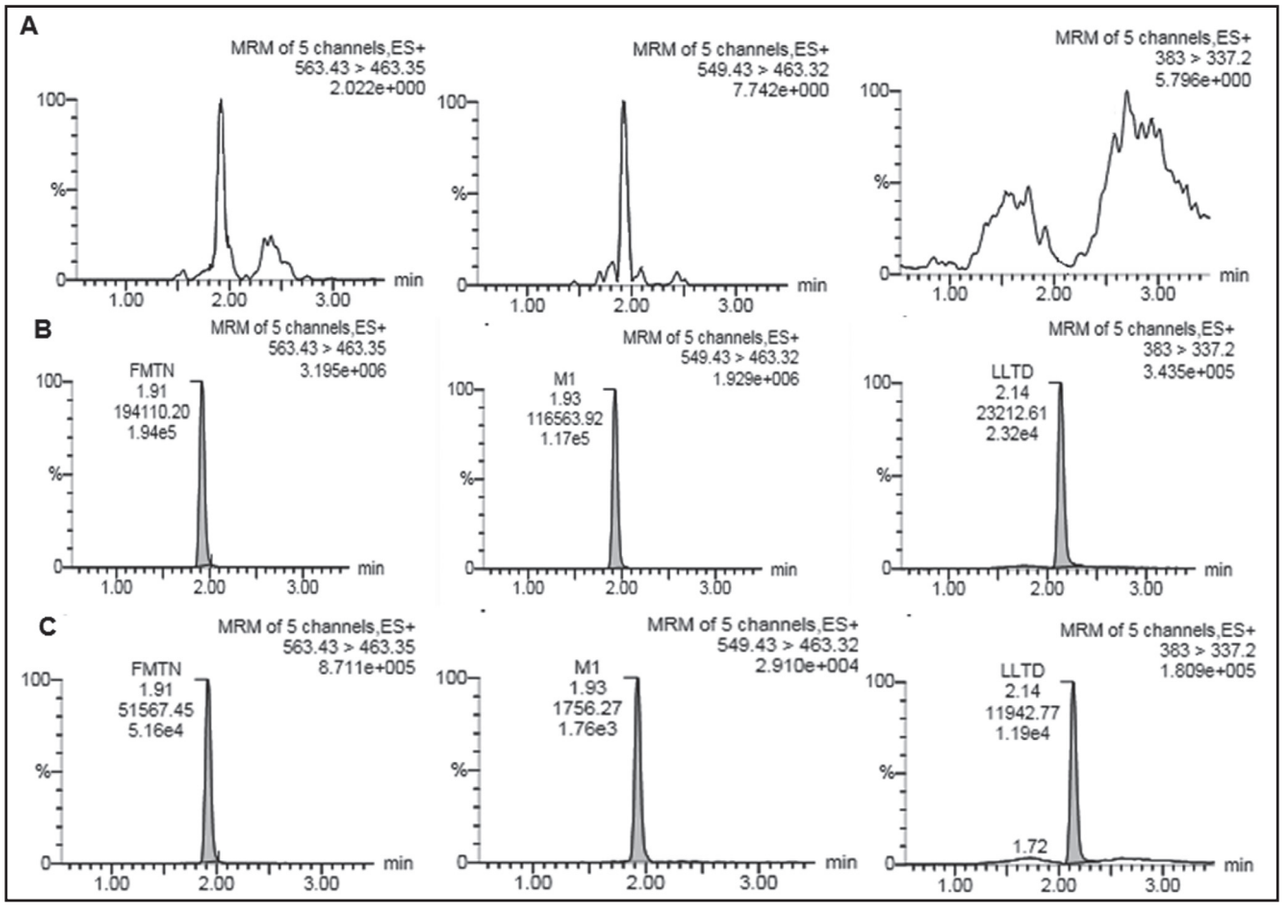

Fig. 2: Chromatograms of flumatinib, M1 and the internal standard loratadine. A) blank plasma; B) QC sample with 100 ng/mL of flumatinib and M1; C) a plasma sample obtained from a rat at 12 h after administration of 40 mg/kg flumatinib.

tion coefficients r = 0.9998 and 0.9998, respectively. According to the working curve, the linear range of M1 in liver microsomes is 1.0~250 ng/mL with correlation coefficient r = 0.9903. The slope values were consistent when evaluated by weighted ($1/x^2$) linear regression.

2.1.3. Precision and accuracy

The results showed that the intra-day RSD% of flumatinib in rat plasma was between 0.78 and 3.3%, and the RE% was -2.6 to 1.2%; the intra-day RSD% of M1 in rat plasma was 0.99 to 3.6%, and the RE% was -3.2 to 6.9%. The intra-day RSD% of M1 in liver microsomes was 0.24 to 1.8%, and RE% was -10.7 to 9.2%. All indicators met the requirement that the precision (RSD%) and accuracy (RE%) should both be less than 15%.

Table 1: The metabolites obtained by incubation of flumatinib with HLM and human recombinant cytochrome P450 enzymes

Enzymes	Metabolites
HLM	M1, M2-1, M2-2, M2-3, M2-4, M2-9
CYP2C8	M1, M2-1, M2-9
CYP 1A2	M2-1
CYP 3A4	M1, M2-1, M2-2, M2-3, M2-4, M2-9
CYP 2C19	M1
CYP 2D6	M1, M2-1
CYP 2C9	M1, M2-1, M2-3
CYP 2B6	M1, M2-3

2.2. Enzyme kinetic profiles

The metabolites obtained following the incubation of flumatinib with liver microsomes were M1, M2-1, M2-2, M2-3, M2-4, and M2-9 (Table 1). The peak area of metabolites indicated that M1, M2-4, and M2-9 were major metabolites after incubation of flumatinib with liver microsomes; hence, we investigated these three metabolites in enzyme kinetic studies. As shown in Table 1, M1 is the product of flumatinib metabolism catalyzed by 6 recombinant CYP enzymes, except CYP1A2. The metabolites produced by human recombinant CYP3A4 are similar to those of human liver microsomes. Among the seven recombinant enzymes, CYP3A4 produced the most abundant metabolites, followed by CYP2C8.

In enzyme kinetic studies, kinetic curves (Fig. 3) and main enzyme kinetic parameters (Table 2) of liver microsomes and different enzyme subtypes (CYP3A4 and CYP2C8) were determined over a flumatinib concentration range of 0–250 μM. As shown in Table 2, M2-4 and M2-9 were mainly mediated by CYP3A4, while M1 was mediated concurrently by CYP3A4 and CYP2C8. The enzyme kinetic parameters indicated that CYP2C8 had stronger ability to produce M1 than that of CYP3A4, but CYP3A4 had dramatically stronger ability to produce M2-4 and M2-9 than that of CYP2C8. However, considering the high expression of CYP3A4 in the liver, these findings suggested that CYP3A4 plays a predominant role in the metabolism of flumatinib in human body.

2.3. Metabolic inhibition

The contributions of CYP3A4 in the metabolism of flumatinib were further evaluated using three drugs (erythromycin, cyclosporine, and voriconazole), all of which are CYP3A4 specific inhibitors. When flumatinib was co-incubated with human liver microsomes

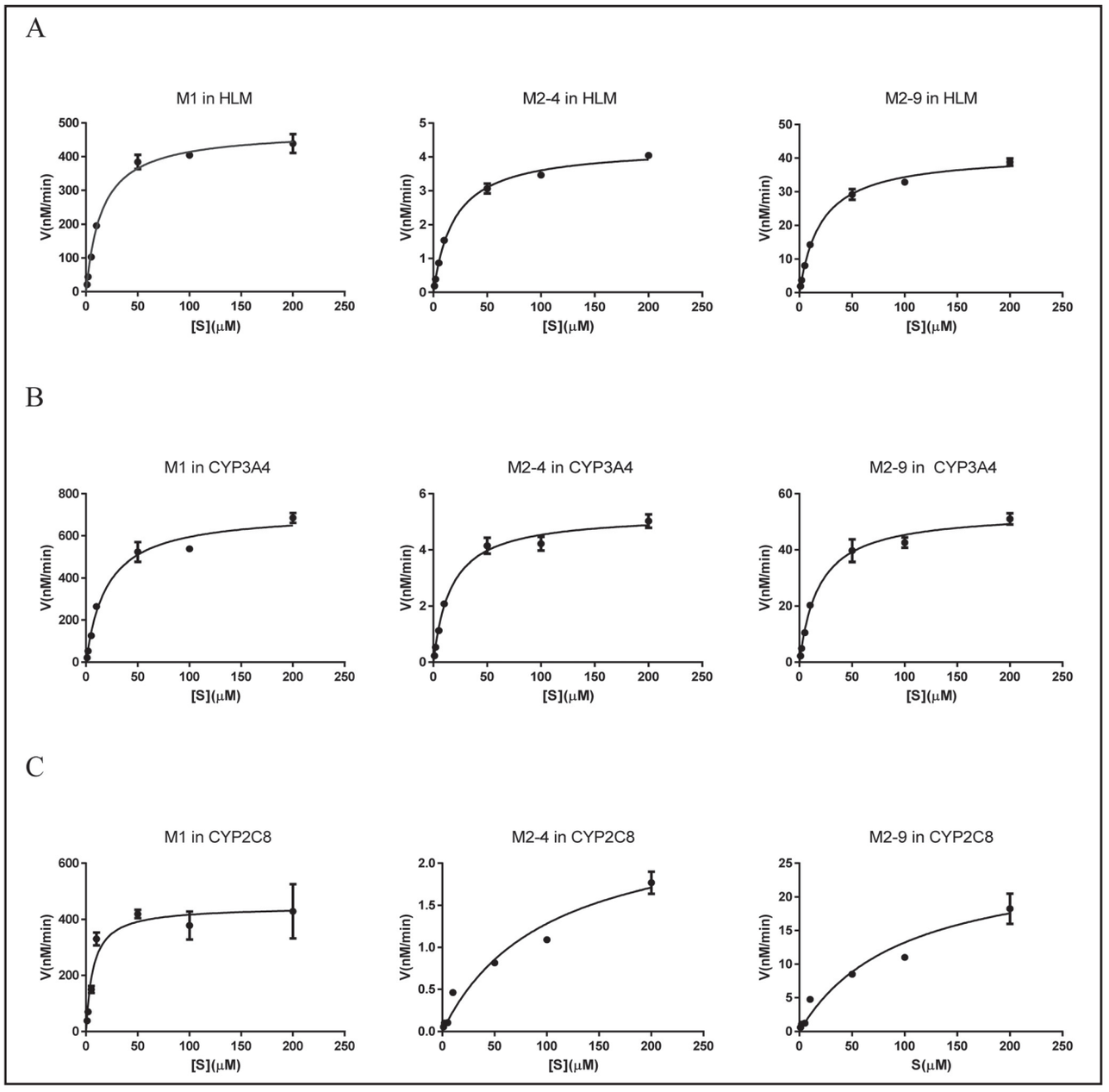

Fig. 3: Kinetic curves of M1, M2-4 and M2-9 in different enzyme subtype incubations. A) human liver microsome; B-CYP3A4; C) CYP2C8.

and human recombinant CYP3A4, all three drugs suppressed the metabolism of flumatinib, and the effects on enzyme metabolism are shown in Fig. 4A and 4B. The concentrations of the three metabolites, M1, M2-4, and M2-9, were significantly decreased, further indicating that flumatinib is mainly metabolized by CYP3A4. In addition, no significant inhibitory effect was observed in the CYP2C8 incubation system (Fig. 4C).

2.4. Pharmacokinetic study

The plasma concentration-time curves of flumatinib and M1 after a single intragastric administration of flumatinib in rats are shown in Fig. 5. The non-compartmental model of the DAS 3.3.1 software was used to calculate the main pharmacokinetic parameters of flumatinib and M1. As shown in Table 3, the AUC and C_{max}

Table 2: Enzyme kinetic parameters of metabolites of flumatinib in HLM and human recombinant cytochrome P450 enzymes

Enzyme	M1			M2-4			M2-9		
	V_{max} (nM/min)	K_m (μM)	CL_{int} (mL/min)	V_{max} (nM/min)	K_m (μM)	CL_{int} (mL/min)	V_{max} (nM/min)	K_m (μM)	CL_{int} (mL/min)
HLM	479±14	15.6±1.7	30.7	4.30±0.09	19.5±1.5	0.22	41.4±1.0	20.5±1.8	2.02
CYP3A4	714±30	20.1±3.2	35.5	5.28±0.18	16.5±2.2	0.32	53.7±1.9	18.6±2.5	2.89
CYP2C8	446±31	6.90±2.06	64.6	2.57±0.36	100±31	0.03	26.2±4.3	98.0±36.0	0.27

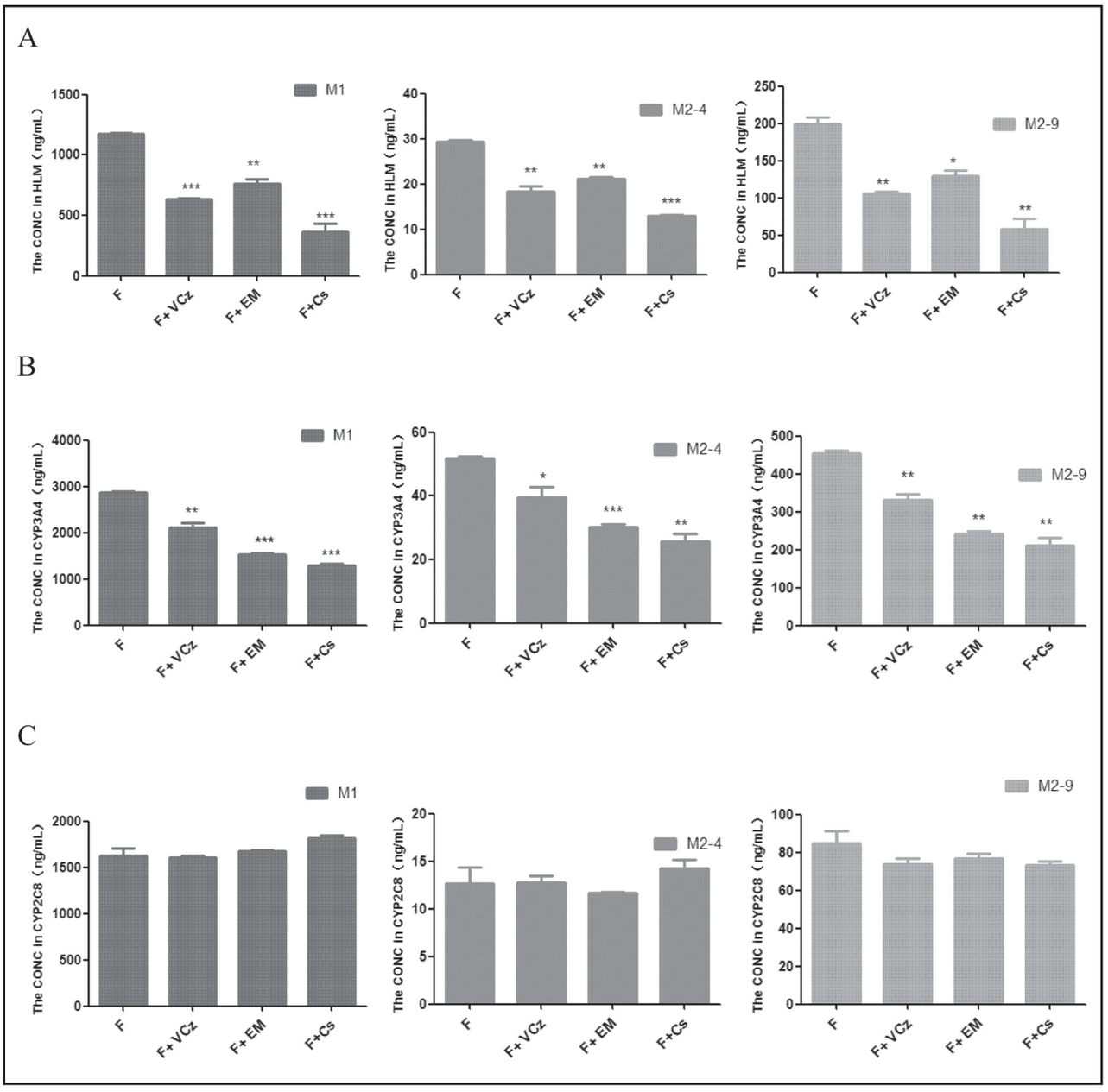

Fig. 4: The inhibitory effect of antibiotics on the formation of M1, M2-4 and M2-9. A) human liver microsome; B) CYP3A4; C) CYP2C8. F, flumatanib; VCz, voriconazole; EM, erythromycin; Cs, cyclosporine.

Table 3: Plasma pharmacokinetic parameters of flumatinib in rats (n = 6)

Parameters	Flumatinib	Flumatinib+ erythromycin	*t*-test	Flumatinib+ cyclosporine	*t*-test	Flumatinib+ voriconazole	*t*-test
AUC_{0-t} (μg /L·h)	3572±401	8111±2333	***	11251±4986	**	5634±2389	n.s.
$AUC_{0-\infty}$ (μg/L·h)	3589±407	8111±2333	***	11269±4996	**	5643±2386	n.s.
$MRT_{(0-t)}$	5.70±0.55	6.33±0.72	n.s.	7.02±1.27	*	6.37±0.57	n.s.
$MRT_{(0-\infty)}$	5.89±0.76	6.33±0.72	n.s.	7.10±1.28	n.s.	6.41±0.50	n.s.
T_{max} (h)	2.50±0.84	2.83±0.98	n.s.	3.17±1.60	n.s.	4.17±2.04	n.s.
$T_{1/2}$ (h)	4.33±2.76	2.79±0.305	n.s.	4.55±2.08	n.s.	2.77±0.27	n.s.
Vz/F	54.5±14.6	22.0±9.2	**	19.8±5.8	***	32.2±11.5	n.s.
CLz/F	11.3±1.4	5.34±1.75	***	4.24±1.89	***	8.03±2.80	n.s
C_{max} (μg/L)	865±170	1129±125	***	1246±147	***	746±293	n.s.

Note: n.s. means no significance
*, $P< 0.05$; **, $P< 0.01$; ***, $P< 0.001$vs the control group

Table 4: Plasma pharmacokinetic parameters of M1 in rats (n = 6)

	Flumatinib	Flumatinib+ erythromycin	*t*-test	Flumatinib+ cyclosporine	*t*-test	Flumatinib+ voriconazole	*t*-test
AUC_{0-t} (μg /L·h)	465±123	604±220	n.s.	546±170	n.s.	222±121	**
$AUC_{0-\infty}$ (μg/L·h)	487±127	608±225	n.s.	561±183	n.s.	236±122	**
$MRT_{(0-t)}$	6.65±1.27	8.86±2.40	n.s.	6.69±1.13	n.s.	5.47±0.75	n.s.
$MRT_{(0-\infty)}$	8.24±1.74	8.84±2.61	n.s.	7.26±1.49	n.s.	6.42±0.95	*
T_{max}(h)	2.08±1.11	3.33±1.63	n.s.	3.83±1.17	*	3.00±0.89	n.s.
$T_{1/2}$(h)	8.32±3.53	5.15±2.52	n.s.	3.86±1.27	*	3.48±1.00	**
Vz/F	994±362	489±161	*	405±110	*	852±349	n.s.
CLz/F	86.7±21.6	74.2±28.3	n.s.	77.3±22.7	n.s.	234±86	*
C_{max}(μg/L)	81.6±12.8	76.3±19.5	n.s.	71.3±30.8	n.s.	41.8±19.0	**

Note: n.s. means no significance
*, $P< 0.05$; **, $P< 0.01$

values of flumatinib in erythromycin and cyclosporine co-administered groups were both significantly increased compared with individual treatment group, and the Vz/F and CLz/F values of flumatinib in erythromycin and cyclosporine co-administered groups were both significantly decreased compared with flumatinib individual treatment group. The AUC values of voriconazole and flumatinib co-administered group were slightly increased and the Vz/F and CLz/F values were slightly decreased compared with the flumatinib individual treatment group. These results suggest that when flumatinib is co-administered with cyclosporine and erythromycin, the pharmacokinetic parameters of flumatinib may change significantly *in vivo*. However, the pharmacokinetic parameters of M1 of co-administered groups compared with those of the flumatinib individual treatment group did not show consistent results (Table 4).

2.5. Conclusions

In conclusion, we found that CYP3A4 and CYP2C8 were the main cytochrome P450 enzyme substyles catalyzing the metabolism of flumatinib, and CYP3A4 has a stronger metabolic ability for flumatinib than CYP2C8. Erythromycin, cyclosporine, and voriconazole can inhibit the metabolism of flumatinib in *in vitro*. Meanwhile, co-administration of erythromycin and cyclosporine with flumatinib increased the plasma concentration and the systemic exposure of flumatinib in rats, which indicated that lower doses should be considered in clinical practice.

3. Experimental

3.1. Materials

Human-recombinant-cytochrome P450 enzymes were purchased from XENOTECH (KS, USA). Pooled human liver microsomes (HLM) were purchased from RILD (Shanghai, China). Flumatinib mesylate and metabolites were provided by Jiangsu Hansoh Pharmaceutical Co. Ltd. (Lianyungang, China). Loratadine (internal standard, IS) were purchased from Aladdin (Shanghai, China). Voriconazole was purchased from Livson Pharmaceutical Co. Ltd. (Zhuhai, China). Erythromycin was purchased from Zhejiang China Resources Sanjiu Pharmaceutical Co. Ltd. (Lishui, China). Cyclosporine was purchased from Novartis Pharma Stein AG (Switzerland). HPLC grade methanol and acetonitrile were purchased from Sigma-Aldrich Chemical Co. Ltd. (St. Louis, MO, USA). HPLC grade ammonium acetate were supplied by Tedia (Fairfield, OH, USA).

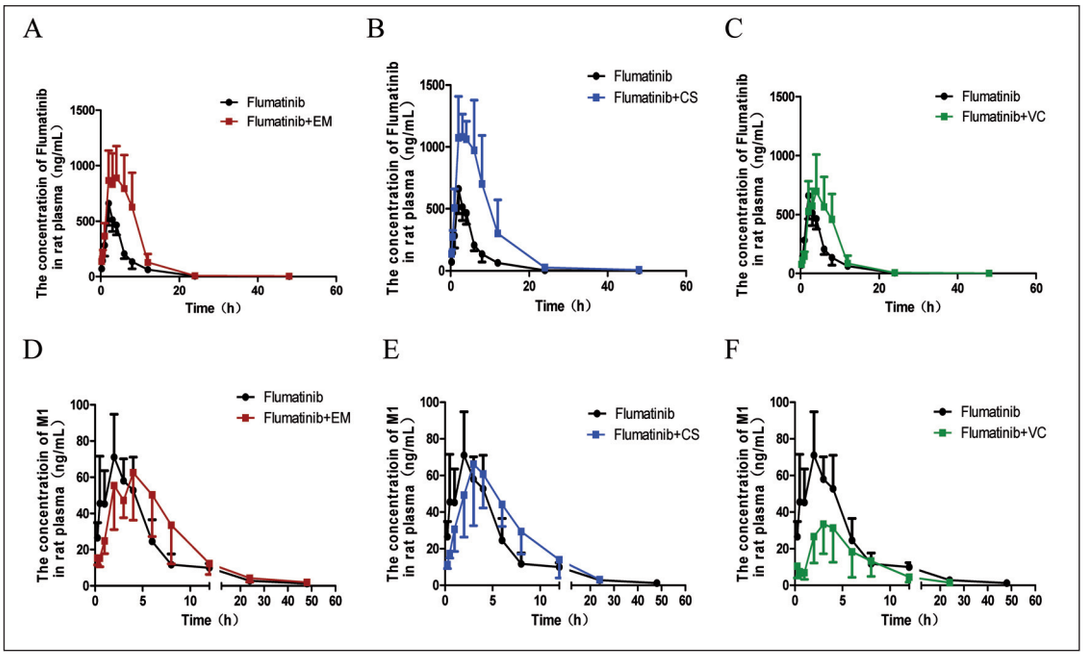

Fig. 5: The plasma concentration-time curves of flumatinib and M1 after a single intragastric co-administration of flumatinib and inhibitors. A. Flumatinib (flumatinib + erythromycin); B. Flumatinib (flumatinib + cyclosporine); C. Flumatinib (flumatinib + voriconazole); D. M1 (flumatinib + erythromycin); E. M1 (flumatinib + cyclosporine); F. M1 (flumatinib + voriconazole).

3.2. Animals

Specific pathogen free Sprague-Dawley (SD) rats were obtained from Zhejiang Academy of Medical Sciences, and maintained at an animal facility according to protocols approved by the Review Committee of Animal Care and Use of Zhejiang University. On arrival, all rats were randomized and divided into four groups, flumatinib group, flumatinib+erythromycin group, flumatinib+cyclosporine group, and flumatinib+voriconazole group. Each group included three male and three female rats. Animals had free access to drink water and diet, under controlled conditions of humidity (50±10 %), light (12/12 hours light/dark cycle), and temperature (25±2 °C). All rats were quarantined for one week before starting the experiment. All animal studies were conducted according to protocols approved by the Review Committee of Animal Care and Use of Zhejiang University and have been carried out in accordance with the Declaration of Helsinki.

3.3. LC-MS/MS analysis

A Waters Acquity UPLC system (Waters, USA) were used for chromatographic separation and detection. The Zorbax SB-Aq column (2.1 mm × 50 mm, 3.5 μm) was used. Flow rate was set at 0.35 mL/min. The mobile phase A consisted of 5 mM ammonium acetate and 0.4% formic acid aqueous solution and mobile phase B of pure methanol. The gradient applied was as follows: 0.00-0.50 min, 20% B; 0.50-1.50 min, 20% B→80% B; 1.50-2.75 min, 80% B→20% B; 2.75-3.50 min, 20% B. The column temperature was set at 30 °C.

Mass spectrometry was performed on a Waters Xevo TQ-S Micro mass spectrometer. All chemicals were detected in the positive ionization mode. The ion source parameters are as follows, capillary voltage was set at 2.50 kV and source temperature at 150 °C, the desolvation gas was nitrogen at a flow rate of 650 L/h and at a temperature of 350 °C, the dwell time was set at 0.065 s, the cone voltage was set at 100 V and the collision voltage was set at 28.0 V for flumatinib, M1 and M2-4, 32.0 V for M2-9, 18.0 V for internal standard, respectively. The multiple reaction monitoring (MRM) transitions for analytes and IS were as follows: *m/z* 563.4→463.3 for flumatinib, *m/z* 549.4→463.3 for M1, *m/z* 579.2→479.1 for M2-4, *m/z* 579.4→461.3 for M2-9, *m/z* 383.0→337.2 for IS, respectively. The structures of flumatinib and its metabolites are shown in Fig. 1.

3.4. Plasma sample preparation

Double-fold acetonitrile was used to precipitate the protein. Supernatant (50 μL) was transferred to a 1.5 mL centrifuge tube, add 2.5 μL of diluent (acetonitrile: water = 1:1, v/v), and add 100 μL internal standard loratadine, dissolved in acetonitrile, at a concentration of 50 ng/mL, vortexed for 3 min, centrifuged at 13,000 rpm for 10 min. Then collected the supernatant, and 5 μL was injected for the analysis of each sample.

3.5. Preparation of working solutions

Stock solutions of 10 mg/mL concentrations of flumatinib, metabolite M1, voriconazole, erythromycin and cyclosporine were prepared by separately dissolving an accurately weighed amount of these compounds in appropriate volumes of DMSO, and stored at -20 °C. Different working solutions were obtained by diluting the stock solutions with acetonitrile/water (1:1, v/v) and store at 4 °C in the dark.

3.6. Method validation

3.6.1. Specificity

In order to assess specificity, the blank plasma sample was prepared as mentioned above (2.4), injected under the LC-MS/MS conditions of this experiment, and the chromatogram of blank plasma was obtained. A certain concentration of flamatinib and concentration gradient of M1 solution was added to the blank plasma, and the corresponding chromatogram was obtained. The corresponding chromatogram of plasma sample which was taken from the rats, 6 h after the administration of flumatinib, was obtained according to the same method. For HLM and human recombinant enzyme samples, a certain concentration of flamatinib and M1 were added, and the corresponding chromatograms were obtained.

3.6.2. Standard curve and linearity

Linearity and calibration curves were obtained by spiking constant volumes of IS (2.5 μL) and different concentrations of standards into 50 μL of blank plasma. Both standards and IS were prepared in a mixture of acetonitrile and water (1:1, v/v). Linearity was studied at different concentration levels. The calibrations were prepared with the following concentrations: 1, 3, 10, 25, 50, 100, 200, and 250 ng/ mL.

3.6.3. Precision and accuracy

Precision (%CV) and accuracy (%RE) were calculated with three spiked replicates of each QC control in one batch during the same day.

3.7. Enzyme kinetic study

Human liver microsomes and human recombinant enzyme subtypes were taken separately at an appropriate amount, diluted to 44.5 μL with phosphate buffer, 0.5 μL of standard solution was added, and vortexed for 5 s. After preheating for 5 min in a 37 °C water bath, 5 μL of 10 mM NADPH solution was added, vortexed for 5 s and then incubated for 30 min in a 37 °C water bath. After the reaction was completed, the protein was treated with two times the amount of acetonitrile (containing 50 ng/mL of internal standard), 2.5 μL of the diluent (acetonitrile: water = 1:1, v/v), and then the internal standard solution was added to 100 μL. The mixture was vortexed for 3 min, and was centrifuged at 13,000 rpm for 10 min. Then collected the supernatant, and 5 μL was injected for the analysis of each sample.

3.8. Pharmacokinetic study

In the pharmacokinetic study, flumatinib was administered to rats alone or together with erythromycin, cyclosporine and voriconazole. In the flumatinib group, each rat received 40 mg/kg of flumatinib. In the flumatinib+erythromycin group, each rat received 40 mg/kg of flumatinib and 50 mg/kg of erythromycin. In the flumatinib+cyclosporine group, each rat received 40 mg/kg of flumatinib and 40 mg/kg of cyclosporine. In the flumatinib+voriconazole group, each rat received 40 mg/kg of flumatinib and 60 mg/kg of voriconazole. The chemicals were administered by gavage. The rats were fasted for more than 12 h until 4 h after the administration, but had free access to drinking water. The blood samples were collected from the tail vein and anticoagulated with heparin sodium at the following times: 0.25, 0.5, 1, 2, 3, 4, 6, 8, 12, 24, and 48 h before and after administration. After collection, each blood sample was immediately centrifuged at 3,500 g for 5 min at 4 °C, and 50 μL of plasma was transferred into a 1.5 mL centrifuge tube and then stored at −80 °C until analysis.

3.9. Data analysis

All assay data was collected and processed by MassLynx software, and data was calculated and processed using Microsoft Excel and Prism 5.0. Since there's no available products on the market, the concentration of M2-4 and M2-9 was calculated according to the stand curve of M1. The concentration-time data was calculated using the DAS 3.3.1 pharmacokinetic software with the statistical moment method. The main pharmacokinetic parameters $AUC_{(0-t)}$, $AUC_{(0-\infty)}$, C_{max}, $t_{1/2}$ of flumatinib and M1 were given.

Funding: This study was supported by the grants from the Ningbo Natural Science Foundation (2017A610257) and the Research Fund for Hospital pharmacy of Zhejiang Pharmaceutical Association (2016ZYY25).

Conflicts of interest: The Authors did not report any conflict of interests.

References

Asada N, Uryu H, Koseki M, Takeuchi M, Komatsu M, Matsue K (2006) Successful treatment of breakthrough Trichosporon asahii fungemia with voriconazole in a patient with acute myeloid leukemia. Clin Infect Dis 43: 39–41.

Bandettini R, Castagnola E, Calvillo M, Micalizzi C, Ravegnani M, Pescetto L, Manzitti C, Soro O, Ricagni L, Lanino E, Miano M, Cuzzubbo D, Conte M, Morreale G, Faraci M (2009) Voriconazole for cryptococcal meningitis in children with leukemia or receiving allogeneic hemopoietic stem cell transplant. J Chemother 21: 108–109.

Gong A, Chen X, Deng P, Zhong DF (2010) Metabolism of flumatinib, a novel antineoplastic tyrosine kinase inhibitor, in chronic myelogenous leukemia patients. Drug Met Dispos 38: 1328–1340.

Gupta A, Punatar S, Gawande J, Mathew L, Kannan S, Khattry N (2017) Analysis of factors affecting initial cyclosporine level and its impact on post transplant outcomes in acute leukemia. J Cancer Res Ther 13: 981–988.

Li Z, Meng L, Zhang YL, Zhu HL, Cui JW, Sun AN, Hu Y, Jin J, Jiang H, Zhang X., Li Y, Liu Q, Liu L, Zhang W, Gu J, Qiao JH, Liu B, Zhang F, Guo Y, Wang J (2019) Frontline flumatinib versus imatinib in patients with chronic myeloid leukemia in chronic phase: results from the China randomized phase III study. J Clin Oncol 37: 7004.

Luo H, Quan H, Xie C, Xu Y, Fu L, Lou L (2010) HH-GV-678, a novel selective inhibitor of Bcr-Abl, outperforms imatinib and effectively overrides imatinib resistance. Leukemia 24: 1807–1809.

Reich C (1954) Erythromycin as an aid in the management of aleukemic myeloblastic leukemias. NY State J Med 54: 2208–2209.

Yang Y, Liu K, Zhong D, Chen X (2012) Simultaneous determination of flumatinib and its two major metabolites in plasma of chronic myelogenous leukemia patients by liquid chromatography–tandem mass spectrometry. J Chromatogr B Analyt Technol Biomed Life Sci 895-896: 25–30.

Yano K, Fujisawa S, Matsui H, Yamamoto Y, Iijima K, Nakano Y (1996) Emergence of nonalbicans Candida species in immunocompromised leukemia patients during fluconazole treatment. J Infect Chemother 2: 268–270.

Yao X, Du N, Hu S, Wang L, Gao J (2019) Rapid advances in research on and development of anticancer drugs in China. Biosci Trends 13: 461–463.

Zhao J, Quan H, Xu Y, Kong X, Jin L, Lou L (2014) Flumatinib, a selective inhibitor of BCR-ABL/PDGFR/KIT, effectively overcomes drug resistance of certain KIT mutants. Cancer Sci 105: 117–125.